Hybrid master oscillator power amplifier system providing 10 mJ, 32 W, and 50 MW pulses for optical parametric chirped-pulse amplification pumping

Andreas Vaupel,[1,2,*] Nathan Bodnar,[1] Benjamin Webb,[1] Lawrence Shah,[1] Michaël Hemmer,[3] Eric Cormier,[2] and Martin Richardson[1]

[1]*Townes Laser Institute, CREOL—The College of Optics and Photonics, University of Central Florida, 4000 Central Florida Blvd., Orlando, Florida 32816, USA*
[2]*Université de Bordeaux—CNRS-CEA, Centre Lasers Intenses et Applications (CELIA), 351 cours de la Libération, F-33405 Talence, France*
[3]*ICFO—Institut de Ciences Fotoniques, Parque Mediterrano de la Technologia, 08860 Castelldefels (Barcelona), Spain*
**Corresponding author: vaupel@creol.ucf.edu*

Received July 10, 2013; revised October 31, 2013; accepted October 31, 2013; posted November 1, 2013 (Doc. ID 193286); published November 21, 2013

We present a high-energy, high-average-power picosecond laser system based on a hybrid chain in a master oscillator power amplifier configuration. The chain is seeded by a Ti:sapphire oscillator, followed by a Yb-doped fiber preamplifier, a Nd:YAG-based regenerate amplifier, and a Nd:YVO_4-based single-pass amplifier. The final diode-pumped, solid-state amplifier is detailed and produces pulses with more than 10 mJ energy at 32 W average power with 207 ps duration, corresponding to 50 MW peak power. The picosecond pulse output is seeded and optically synchronized with the sub-5-fs oscillator for optical parametric chirped-pulse amplification pumping.

OCIS codes: (140.0140) Lasers and laser optics; (140.3280) Laser amplifiers; (140.3530) Lasers, neodymium; (140.3580) Lasers, solid-state; (320.7160) Ultrafast technology.
http://dx.doi.org/10.1364/JOSAB.30.003278

1. INTRODUCTION

Recent advances in optical parametric chirped-pulse amplification (OPCPA) have initiated multiple efforts to develop high-average-power and high-peak-power pump lasers. The OPCPA architecture allows the transfer of energy from a high-energy pulse with picosecond duration to an ultrabroadband chirped pulse. This amplified broadband pulse can subsequently be compressed to sub-10-fs duration, resulting in high-energy few-cycle pulses. The OPCPA process is currently primarily limited in terms of output pulse energy and repetition rate by the performance of picosecond pump laser systems. To date, the record levels for table-top scale, few-cycle OPCPA systems are a peak power of 16 TW [1] and an average power of 22 W [2], while the current record peak power produced by the OPCPA method in general is 0.56 PW corresponding to 38 J pulse energy and 43 fs duration [3].

Several novel high-peak-power and high-average-power OPCPA pump architectures have been developed over the last decade using a range of optical amplifier technologies. Operating with high energy and high peak power, a Yb:YAG thin-disk regenerative amplifier system has been presented with 25 mJ, 1.6 ps, 3 kHz, and 75 W [4], and a Yb:YAG slab produced 20 mJ, 0.83 ps, 12.5 kHz, and 250 W average power [5]. In addition, cryogenically cooled, Yb-based amplifiers show high potential to generate picosecond pulses with ultrahigh power and high pulse energy while maintaining good beam quality. For example, a total-reflective mirror configuration has been reported with an output power of up to 273 W (cw) and 65% optical efficiency [6]. In pulsed operation, cryogenically cooled systems have been used to produce pulses with 120 mJ energy and 70 ns duration at 500 Hz repetition rate [7]. Interesting for OPCPA are picosecond pump laser systems, such as a system producing 13.2 mJ pulse energy with an (uncompressed) transform-limited duration of 15 ps at 1 kHz repetition rate [8] or even 1 J pulse energy and 5 ps duration at 100 Hz [9]. At ultrahigh average powers, amplifiers based upon cryogenically cooled Yb:YAG disks have been employed to generate up to 758 W average power with 15.2 μJ pulse energy and 12.4 ps duration [10]. These systems are able to produce ultrahigh average powers due to the reduced impact of thermally induced aberrations in thin-disk and slab scheme architecture and/or cryogenic cooling. Additionally, the use of Yb amplifiers and chirped-pulse amplification (CPA) enables >GW peak power generation; however, the implementation of CPA for pump generation can significantly increase the overall system complexity and footprint. For example, a Yb-based CPA system was presented producing pulses with 200 mJ energy and 1 ps duration at 10 Hz repetition rate corresponding to 20 W average power [11]; however, the comparatively large footprint (compressor footprint: 6.5 m × 1.5 m × 0.7 m) and long optical path lengths (eight reflections of the compressor gratings with separation of 6 m)

result in non-negligible synchronization jitter for the OPCPA application [12].

The system presented here is based on a master oscillator power amplifier (MOPA) configuration with diode-pumped, solid-state laser (DPSSL) technology. Extracting high energy from MOPA, picosecond, kilohertz DPSSLs can be challenging due to the high peak power, considerable thermally induced effects, and relatively low gain. Examples illustrating the performance of MOPA DPSSL systems include 33.7 W average power at 20 kHz repartition rate with ~220 ps pulse duration corresponding to 7 MW peak power [13] and 0.6 mJ pulse energy and 12 ps duration corresponding to an average/peak power between 46 W/38 MW and 30 W/50 MW based on Nd:YVO_4 [14]. Recently, a system based upon quasi-cw pulsed Nd:YAG amplifier modules was reported producing 90 ps pulses with 130 mJ energy at subkilohertz repetition rate corresponding to 39 W average/2.0 GW peak power [15]. A system, similar to that described in this work, was reported in [16], producing 40 mJ, 48 ps, and 40 W average power with consecutive monolithic Nd:YAG amplifier stages. In this work, we describe in detail a novel system using a hybrid ultrafast/fiber/DPSS architecture seeded by and synchronized to a sub-5-fs oscillator at kilohertz repetition rates. To complete this overview, MOPA DPSSLs have also been employed to generate longer pulse durations (>10 ns). One such system generated up to 1.36 kW average power with a maximum pulse energy of 250 mJ corresponding to 24 MW peak power [17].

The hybrid picosecond DPSS MOPA system presented here represents a novel and compact architecture (overall system size: $3 \times 0.8 \times 0.2$ m^3). The booster amplifier stage is DPSSL based and operates in a similar regime as some of the previously mentioned MOPA systems [13,14,17], but simultaneously offering more than 10 mJ pulse energy, 30 W average power, and 50 MW peak power at kilohertz repetition rates. This system is optically synchronized with a sub-5-fs oscillator and will be used as a pump system for our OPCPA facility HERACLES [18], which is designed to provide few-cycle pulses in the visible/NIR with high pulse energy, kilohertz repetition rate, and more than 1 W average power.

HERACLES performance is expected to be similar to other reported OPCPA systems using "long" picosecond pump pulses, such as a Nd:YAG-based system operating at 78 ps (after frequency doubling to 532 nm) [1] and a Ti:sapphire-based system at 100 ps (after frequency doubling to 400 nm) [19]. The anticipated output is 0.6 mJ pulse energy with 1.8 W average power at 800 nm center wavelength given 10 mJ pump energy at 1064 nm. Increasing the pulse energy from OPCPA systems beyond the millijoule level while maintaining the >1 kHz repetition rate seems feasible with our DPSS approach, in addition to the systems mentioned in [4,5,16].

2. HYBRID ULTRAFAST/FIBER/SOLID-STATE AMPLIFIER CHAIN

The MOPA system presented here is an upgraded second-generation version of our previous system [20], which produced 880 μJ at 2 kHz or 500 μJ at 10 kHz. Similar to [20], an ultrabroadband, few-cycle Ti:sapphire oscillator (Octavius-85M, MenloSystem, Inc.) is used as the front end and provides a seed at 1064 nm to optically synchronize the pump with the pulse to be amplified in the OPCPA. The seed is first amplified to 0.85 mW, 10 pJ at 85 MHz in a fiber amplifier, consisting of 5 m, single-mode, Yb-doped fiber (Nufern, Inc., PM-YSF-HI) pumped by up to 1 W optical power (AlfaLight, Inc., AM4-976A-10-253), a 3 nm bandpass filter centered at 1064 nm (NovaWave Technologies, PMBP-06-N-B-Q), and optical isolators (OFR Thorlabs Inc., IO-L-T980/I1053-65), which is similar to [21]. Amplified spontaneous emission (ASE), in Yb-doped fiber centered at 1030 nm, is minimized by the optical isolators and the 3 nm bandpass filter centered at 1064 nm, such that the ASE is ~50 μW. After this fiber stage, an electro-optic pulse picker (Quantum Technology, Inc., RT-3 and StarFire 2DR-25K-TX-15V) reduces the repetition rate to the 1–5 kHz range before seeding a regenerative amplifier. In comparison to [20], the regenerative amplifier is modified to provide higher pulse energies at 3 kHz repetition rate and is followed by a single-pass booster amplifier (Fig. 1).

The regenerative amplifier is based on a diode-pumped, Nd:YAG ([111]) amplifier module (Northrop Grumman Cutting Edge Optronics, RBA24-1C2) with 2 mm diameter aperture and 73 mm rod length, which is side pumped (cw) by up to 240 W at 808 nm wavelength along the central 4 cm length of the rod. This regenerative amplifier produces ~2 mJ pulse energy (the saturation fluence is ~21 mJ) at 1 kHz, ~1.5 mJ (1.7% rms noise) at 3 kHz, or ~0.8 mJ at 5 kHz. A volume Bragg grating (VBG) (OptiGrate, Corp.) narrows the spectral bandwidth in the regenerative amplifier to the 10-pm-linewidth level and thereby produces a transform-limited duration of 200 ps (FWHM) similar to [20,22]. In the current configuration, the 200 ps pulse duration is seen as a trade-off, similar to other MOPA systems [1,13,16,19,23,24], between a long pulse duration (several nanoseconds) for efficient power extraction from the solid-state amplifiers and the OPCPA application with an optimum duration of less than 100 ps. This duration remains constant throughout the MOPA chain, providing the opportunity to shorten (or lengthen) the duration of the output pulses by replacing the intracavity VBG with one having a wider (or narrower) bandwidth. Operating with picosecond pulse durations assumes high intensities in the solid-state amplifiers exceeding 1 GW/cm^2. For sub-100-ps pulses and good beam quality, we deem an intensity of 4 [1,16] to 6 GW/cm^2 [23] as safe, while the damage threshold is ~7 GW/cm^2 for 200 ps pulses following the empirical square root scaling law [25] based upon an anticipated damage threshold of 10 J/cm^2 for 10 ns pulses (specification from Northrop Grumman Cutting Edge Optronics). As a consequence, the operational fluences in the solid-state amplifiers are determined by the damage threshold, which is below the saturation fluence.

A diode-pumped Nd:YVO_4 amplifier module (Northrop Grumman Cutting Edge Optronics, RBAM20-1C2) with

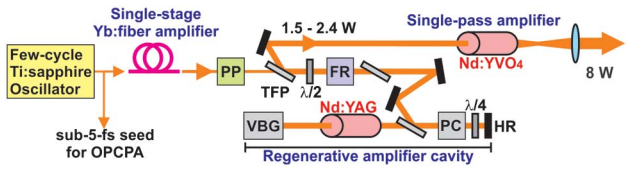

Fig. 1. Schematic of the hybrid ultrafast/fiber/solid-state system with optically synchronized high-energy and high-average-power picosecond pump beam with the femtosecond seed. List of acronyms: PP, pulse picker; TFP, thin-film polarizer; $\lambda/2$, half-wave plate; FR, Faraday rotator; HR, highly reflective mirror; PC, Pockels cell; $\lambda/4$, quarter-wave plate; VBG, volume Bragg grating.

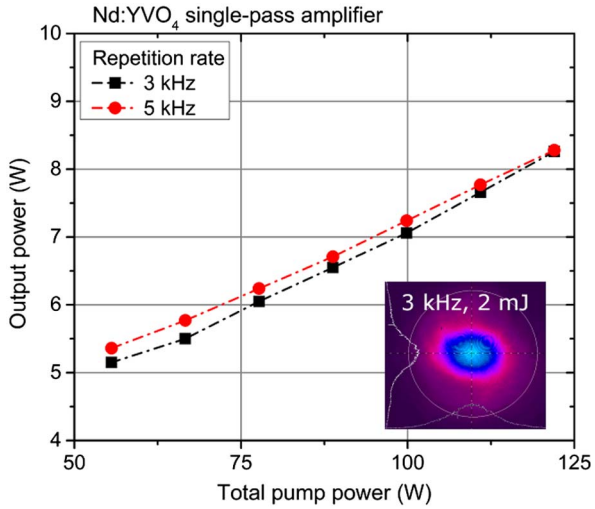

Fig. 2. Amplification characteristics of the single-pass amplifier based on 2 mm diameter Nd:YVO_4 seeded by the regenerative amplifier based on Nd:YAG. The typical output beam profile is shown in the inset.

2 mm diameter and 40 mm length, which is side pumped (cw) by up to 180 W at 808 nm wavelength along the central 3 cm length of the rod, is utilized in a single-pass amplifier configuration to obtain more than 10 W average power at 3 or 5 kHz. The amplification characteristics are shown in Fig. 2 relative to pumped power. The maximum output energy is 2.75 mJ (the saturation fluence is ~5.1 mJ) at 3 kHz and 1.6 mJ at 5 kHz. The output signal was recorded with a fast photodiode as depicted in Fig. 3, showing a clean signal of the main pulse and a minor postpulse at <2.5% amplitude relative to the main pulse (>40:1 ratio) after 14 ns corresponding to the RA cavity round-trip time. The beam pointing stability of the single-pass output is measured to be <100 μrad (rms).

This system "front end" provides a seed of ~2 mJ pulse energy, 3–5 kHz, and ~200 ps duration with excellent beam profile as well as good temporal contrast. To amplify the output further, a booster stage is implemented using two low-noise, diode-pumped, 3-mm-diameter, 8.3-cm-long, Nd:YAG ([111]) modules (the saturation fluence is ~47 mJ) with curved rod ends (concave 0.5 m radius of curvature), which are side

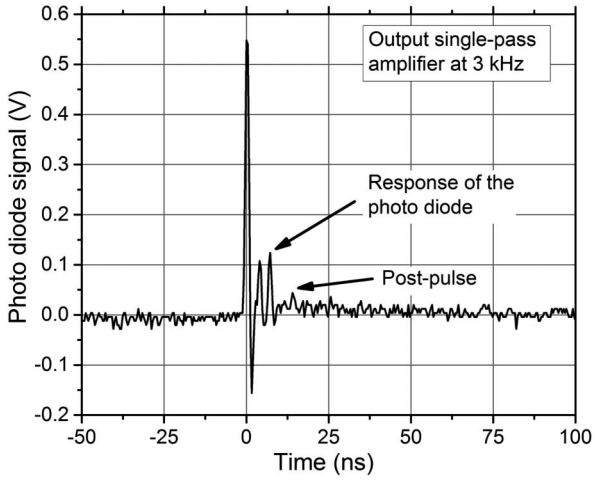

Fig. 3. Output signal of the Nd:YVO_4 single-pass amplifier recorded with a fast photodiode.

pumped (cw) along the central 5 cm of the rod with up to 300 W each at a wavelength of 808 nm (Northrop Grumman Cutting Edge Optronics, SilentLight RBAT35-1C2). A repetition rate of 3 kHz was chosen, since it provides the best compromise between high average power and high pulse energy from the front end as well as the following booster amplifier.

3. MANAGEMENT OF THERMALLY INDUCED EFFECTS IN THE DPSS BOOSTER AMPLIFIER

Amplification of high-energy picosecond pulses with solid-state rod amplifiers is challenging in several ways. First, the high thermal load leads to strong thermal lensing with focal length on the order of ~20 cm. A first-order compensation can be implemented with spherical lenses, where the thermal lensing can be approximately compensated with lens combinations of proper focal length. This compensation is best for the central part of the beam; however, the lensing of the outer part of the beam can deviate strongly from the paraxial case depending on the pump/heat load geometry [17]. It is feasible to compensate higher-order deviations with schemes incorporating a phase conjugating mirror [26], an adaptive mirror [27], or material with opposite thermal response (i.e., opposite dn/dt) [28]. In this work, thermal lens compensation of higher orders is not implemented and therefore acts as nonuniform loss.

Additionally, Nd:YAG under high thermal load suffers from thermally induced depolarization [29], which is typically in the range of 25% for a single amplifier [30] and up to 37% for a configuration consisting of twin Nd:YAG amplifiers [31]. To compensate thermal depolarization, we utilize a 90 deg quartz rotator [32] and a 1:1 relay imaging scheme [33] with twin amplifier modules [31]. A schematic of the booster amplifier scheme is illustrated in Fig. 4, showing the two Nd:YAG modules along with the thermal lensing and depolarization compensation optics.

Thermal lens and depolarization compensation is studied in this system by propagating a low-average-power (0.1 W), 1064 nm, *s*-polarized probe with Gaussian beam distribution in a single-pass configuration through the two identical Nd:YAG amplifiers. Beam profiles after propagation through a polarizer at various angles are shown in Fig. 5. A clear depolarization signature can be identified when no quartz rotator is used, as shown in Fig. 5(a), corresponding to a total depolarization loss of up to 25% and nonuniform spatial distribution. When the 90 deg quartz rotator is used, the depolarization loss is reduced to 5.2% and uniform output beam distribution is obtained, as shown in Fig. 5(b). These residual depolarization losses are a result of the imperfect experimental imaging scheme and the slight differences between the twin amplifiers. Further reduction of the depolarization loss potentially below

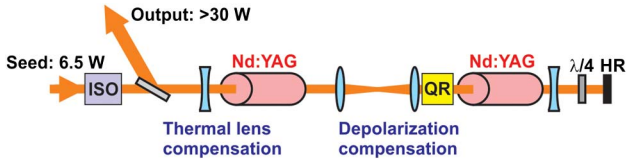

Fig. 4. Schematic of the amplifier stage showing thermal lens and depolarization compensation optics and two identical amplifier modules. List of acronyms: ISO, optical isolator consisting of two TFP, FR, and $\lambda/2$; QR, 90 deg quartz rotator; $\lambda/4$, quarter-wave plate.

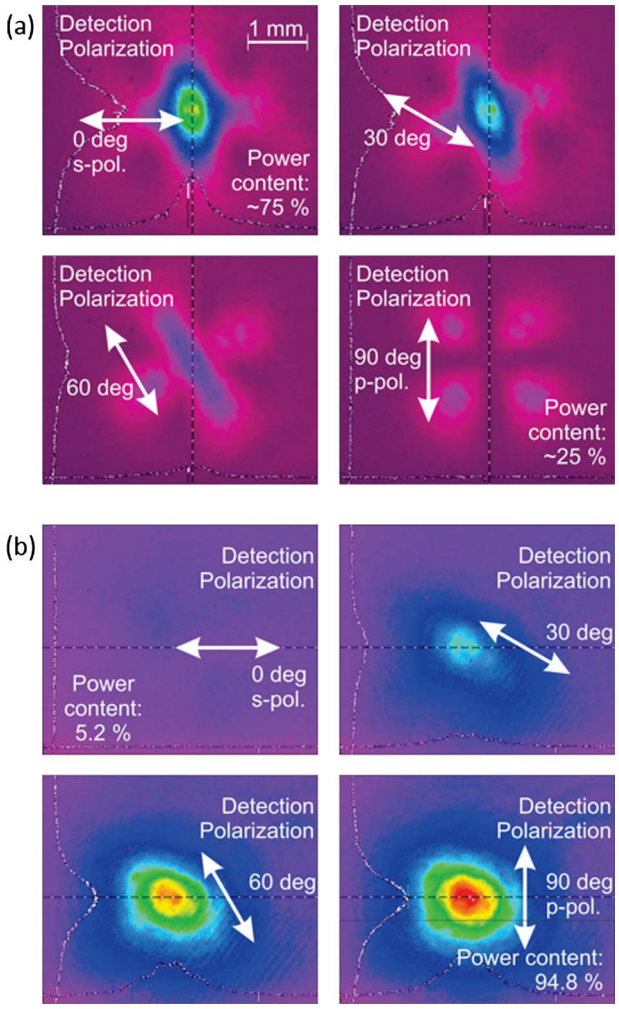

Fig. 5. Observed beam profiles after a single pass through the two identical amplifiers at full thermal load with (a) no quartz rotator and (b) 90 deg quartz rotator. A polarizer was used in front of the beam profiler with indicated direction.

1% could be achieved by utilizing a Faraday rotator instead of a quarter-wave plate [34,35], but was not attempted here.

The Nd:YAG modules employed here offer acceptable gain at few-kilohertz repetition rates depending on the extraction efficiency, repetition rate, fill factor (defined as the ratio of the beam to the rod amplifier cross-sectional area), and operated fluence. The small signal gain is studied in this case again using a low-power, cw probe beam. The gain is 1.81 for the first module and 2.1 for the second module. The corresponding total gain of a single pass through the stage is 3.78 including all optical losses. Double-passing the amplifier stage results in a small signal gain exceeding 11, which is expected to reduce as the gain is saturated.

4. HIGH-ENERGY, HIGH-AVERAGE-POWER PICOSECOND OUTPUT

Proper thermal lens compensation is critical in DPSSLs and generally assumes a fixed thermal load, which depends on the optical pump power as well as the optical extraction efficiency of the amplifier. Thus, a proper thermal lens compensation scheme is only appropriate for a limited range of operating conditions. A change of the thermal lens in the imaging scheme leads inevitably to a diverging (overcompensated) or converging (undercompensated) output beam. If the output beam is diverging (or converging) and if the fill factor is large, the output beam profile often suffers diffraction causing beam quality degradation. However, if the beam is too small, the overall gain is smaller since it is highly dependent on the fill factor. Thus, the output beam profile and gain have to be optimized based on the solid-state rod amplifier configuration and point of operation.

These effects are investigated for the double-passed amplifier stage with low seed power (1 W) far below efficient power extraction or saturation (Fig. 6). Our compensation scheme consists of two negative lenses, each placed symmetrically in front of the first and behind the second amplifier module (similar to [17]), as well as the negatively curved rod ends. The focal length and position of the negative lenses have a significant impact on the obtainable gain. Numerical and experimental investigations of this amplifier stage indicated that the best configuration was to position the lenses 5 cm in front of the first and symmetrically behind the second amplifier (i.e., 8.9 cm from the center of the amplifier) with a focal length of either $f = -30$ or -40 cm. Fine adjustments to the scheme are possible by changing the thermal lenses of the amplifiers (i.e., pump power). Output beam profiles for the case with $f = -40$ cm lenses are shown in Fig. 6. It can be seen that Gaussian beam profiles are obtained for pump powers below 450 W, while the onset of diffraction is observed above 460 W due to undercompensation of the thermal lens. In the case with $f = -40$ cm, the gain increases almost linearly with pump power from 400 to 465 W before rolling over. We attribute the rollover character of the curve to increased optical losses due to the strong thermal lensing and undercompensation, since the gain per amplifier module is expected to increase linearly with pump power in this regime. The largest gain observed was 11.0 at full pump power (490 W) and 9.8 at 460 W. In the case of $f = -30$ cm, the gain increases linearly with a highest obtainable value of 7.2. Considering both effects, a pump power between 440 and 460 W is chosen with $f = -40$ cm corresponding to the shaded area in Fig. 6.

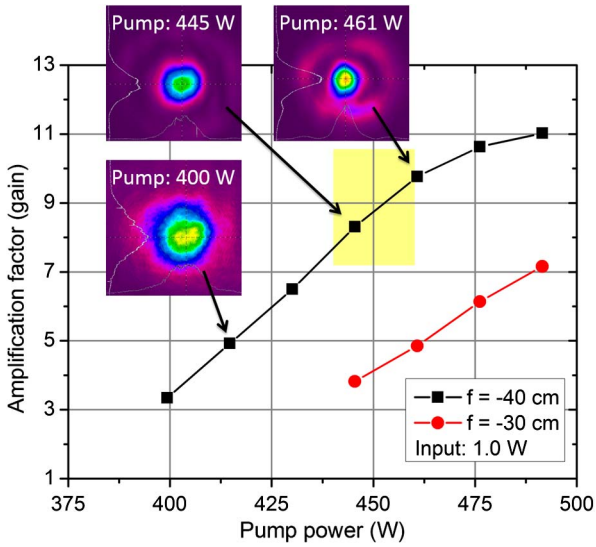

Fig. 6. Influence of the thermal lens compensation scheme on the obtainable amplification gain. Characteristic beam profiles are shown for the case of $f = -40$ cm.

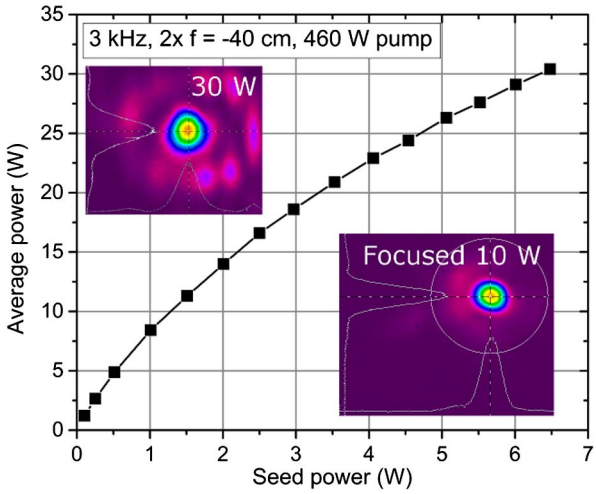

Fig. 7. High-power amplification characteristics of the double-passed booster stage and obtained beam profiles.

After optimization at low seed pulse energy, the amplifier stage is seeded by up to 6.5 W from the Nd:YVO_4 single-pass amplifier and alignment optimized. It was found experimentally that this configuration ($f = -40$ cm) also resulted in the highest output power from the amplifier stage. Figure 7 shows the amplification characteristics for up to 2.15 mJ input pulse energy. The highest recorded average power is 30.3 W (measured with OPHIR LaserStar, OPHIR 30(150)A-SH-V1 ROHS) corresponding to a gain of 4.7. The inset in Fig. 7 shows the measured beam profile at 30 W average power confirming a Gaussian beam distribution for which the thermal lens compensation scheme is optimized. A minor diffraction ring is visible due to imperfect compensation of the thermal lens affecting the outer portion of the beam. No ASE is observed if the seed beam is blocked to the booster amplifier stage, due to the low gain and the distances between the amplifier modules. Furthermore, the regenerative amplifier has low ASE (due to the VBG [20]), and the output pulses of the single-pass show high contrast (>40:1 ratio of main to single postpulse). As such, >97.5% of the total energy is in the main pulse. The highest obtained average power during the experiments was 32.0 W, which at 3 kHz repetition rate corresponds to more than 10 mJ pulse energy. The power stability was measured to be better than 0.5% (rms) at a lower power of 20 W over 15 min.

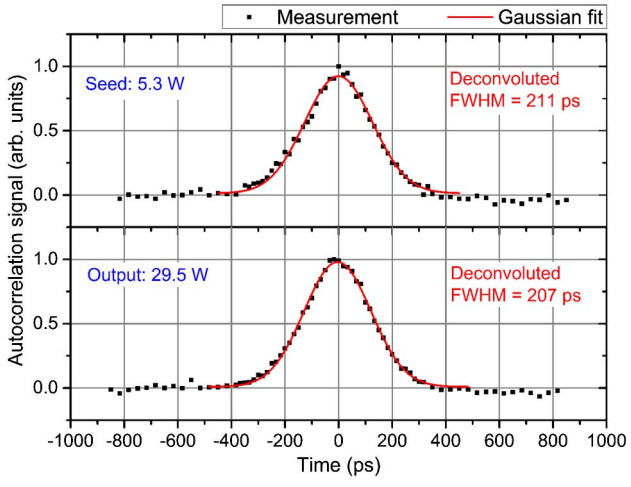

Fig. 8. Measured second-harmonic autocorrelation traces for the seed (top) and amplified pulses (bottom) indicating durations of 211 and 207 ps, respectively.

Intensity autocorrelation traces for seed and amplified pulses are shown in Fig. 8. Pulse durations (FWHM) before and after the amplifier stage of 211 and 207 ps, respectively, are deduced assuming Gaussian pulse shapes in both cases. Given this duration (207 ps) at the highest amplified pulse energy (>10 mJ), the corresponding peak power of the amplified pulses is 50 MW. The operating intensity in the final pass is estimated to be 1.6 GW/cm^2 with a corresponding B-integral of 0.40. Both values are comparable with picosecond solid-state systems based on Nd:YAG [1,16,23]. No fundamental limitations due to damage or nonlinearities have been observed experimentally.

5. SUMMARY

A MOPA system is presented based on a hybrid ultrafast/fiber/solid-state chain producing energetic picosecond pulses with high average power for OPCPA pumping. The amplifier chain consists of a Yb-doped fiber preamplifier, a Nd:YAG-based regenerative amplifier, and a Nd:YVO_4-based single-pass amplifier, and is seeded by a sub-5-fs Ti:sapphire oscillator. The final DPSSL amplifier stage is a double-pass configuration consisting of two identical Nd:YAG amplifier modules with thermal lens and depolarization compensation. The setup was investigated with a cw beam, and key results on small signal gain and depolarization compensation are presented. Further optimization was conducted when seeded with picosecond pulses from the regenerative and single-pass amplifier and high-energy picosecond pulses were obtained with simultaneous high average power. The maximum output is more than 10 mJ pulse energy with up to 32 W average power and 207 ps duration, corresponding to 50 MW peak power and good Gaussian output beam. The system provides simultaneously high energy, high peak power, and high average power and is intended for use as a pump laser for an OPCPA system with kilohertz repetition rates.

ACKNOWLEDGMENTS

This study was funded by the DOE, through an ARO MURI program, and by the State of Florida.

REFERENCES

1. D. Herrmann, L. Veisz, R. Tautz, F. Tavella, K. Schmid, V. Pervak, and F. Krausz, "Generation of sub-three-cycle, 16 TW light pulses by using noncollinear optical parametric chirped-pulse amplification," Opt. Lett. **34**, 2459–2461 (2009).
2. J. Rothhardt, S. Demmler, S. Hädrich, J. Limpert, and A. Tünnermann, "Octave-spanning OPCPA system delivering CEP-stable few-cycle pulses and 22 W of average power at 1 MHz repetition rate," Opt. Express **20**, 10870–10878 (2012).
3. V. V. Lozhkarev, G. I. Freidman, V. N. Ginzburg, E. V. Katin, E. A. Khazanov, A. V. Kirsanov, G. A. Luchinin, A. N. Mal'shakov, M. A. Martyanov, O. V. Palashov, A. K. Poteomkin, A. M. Sergeev, A. A. Shaykin, and I. V. Yakovlev, "Compact 0.56 Petawatt laser system based on optical parametric chirped pulse amplification in KD*P crystals," Laser Phys. Lett. **4**, 421–427 (2007).
4. T. Metzger, A. Schwarz, C. Y. Teisset, D. Sutter, A. Killi, R. Kienberger, and F. Krausz, "High-repetition-rate picosecond pump laser based on a Yb:YAG disk amplifier for optical parametric amplification," Opt. Lett. **34**, 2123–2125 (2009).

5. M. Schulz, R. Riedel, A. Willner, T. Mans, C. Schnitzler, P. Russbueldt, J. Dolkemeyer, E. Seise, T. Gottschall, S. Hädrich, S. Duesterer, H. Schlarb, J. Feldhaus, J. Limpert, B. Faatz, A. Tünnermann, J. Rossbach, M. Drescher, and F. Tavella, "Yb: YAG Innoslab amplifier: efficient high repetition rate subpicosecond pumping system for optical parametric chirped pulse amplification," Opt. Lett. **36**, 2456–2458 (2011).
6. H. Furuse, J. Kawanaka, K. Takeshita, N. Miyanaga, T. Saiki, K. Imasaki, M. Fujita, and S. Ishii, "Total-reflection active-mirror laser with cryogenic Yb:YAG ceramics," Opt. Lett. **34**, 3439–3441 (2009).
7. E. A. Perevezentsev, I. B. Mukhin, I. I. Kuznetsov, O. V. Palashov, and E. A. Khazanov, "Cryogenic disk Yb: YAG laser with 120 mJ energy at 500 Hz pulse repetition rate," Quantum Electron. **43**, 207–210 (2013).
8. K.-H. Hong, J. T. Gopinath, D. Rand, A. M. Siddiqui, S.-W. Huang, E. Li, B. J. Eggleton, J. D. Hybl, T. Y. Fan, and F. X. Kärtner, "High-energy, kHz-repetition-rate, ps cryogenic Yb:YAG chirped-pulse amplifier," Opt. Lett. **35**, 1752–1754 (2010).
9. B. A. Reagan, K. A. Wernsing, A. H. Curtis, F. J. Furch, B. M. Luther, D. Patel, C. S. Menoni, and J. J. Rocca, "Demonstration of a 100 Hz repetition rate gain-saturated diode-pumped table-top soft x-ray laser," Opt. Lett. **37**, 3624–3626 (2012).
10. D. C. Brown, J. M. Singley, K. Kowalewski, J. Guelzow, and V. Vitali, "High sustained average power cw and ultrafast Yb: YAG near-diffraction-limited cryogenic solid-state laser," Opt. Express **18**, 24770–24792 (2010).
11. S. Klingebiel, C. Wandt, C. Skrobol, I. Ahmad, S. A. Trushin, Z. Major, F. Krausz, and S. Karsch, "High energy picosecond Yb:YAG CPA system at 10 Hz repetition rate for pumping optical parametric amplifiers," Opt. Express **19**, 5357–5363 (2011).
12. S. Klingebiel, I. Ahmad, C. Wandt, C. Skrobol, S. A. Trushin, Z. Major, F. Krausz, and S. Karsch, "Experimental and theoretical investigation of timing jitter inside a stretcher-compressor setup," Opt. Express **20**, 3443–3455 (2012).
13. M. Lührmann, C. Theobald, R. Wallenstein, and J. A. L'huillier, "High energy cw-diode pumped Nd:YVO_4 regenerative amplifier with efficient second harmonic generation," Opt. Express **17**, 22761–22766 (2009).
14. C. Heese, A. E. Oehler, L. Gallmann, and U. Keller, "High-energy picosecond Nd:YVO_4 slab amplifier for OPCPA pumping," Appl. Phys. B **103**, 5–8 (2011).
15. D. W. E. Noom, S. Witte, J. Morgenweg, R. K. Altmann, and K. S. E. Eikema, "High-energy, high-repetition-rate picosecond pulses from a quasi-CW diode-pumped Nd:YAG system," Opt. Lett. **38**, 3021–3023 (2013).
16. K. Michailovas, V. Smilgevicius, and A. Michailovas, "Kilohertz rate picosecond pulses amplifier for pumping of OPCPA system," in *Lasers, Sources, and Related Photonic Devices*, OSA Technical Digest (CD) (Optical Society of America, 2012), paper AW4A.3.
17. K. Nicklaus, M. Hoefer, D. Hoffmann, J. Luttmann, R. Wester, and R. Poprawe, "MOPA with kW average power and multi MW peak power: experimental results, theoretical modeling, and scaling limits," Proc. SPIE **6100**, 610016 (2006).
18. M. Hemmer, A. Vaupel, and M. Richardson, "Current status of the HERACLES, a millijoule level, multi kHz, few-cycle, and CEP stabilized OPCPA system," in *Conference on Lasers and Electro-Optics 2010*, OSA Technical Digest (CD) (Optical Society of America, 2010), paper CTuFF5.
19. S. Adachi, H. Ishii, T. Kanai, N. Ishii, A. Kosuge, and S. Watanabe, "1.5 mJ, 6.4 fs parametric chirped-pulse amplification system at 1 kHz," Opt. Lett. **32**, 2487–2489 (2007).
20. M. Hemmer, A. Vaupel, M. Wohlmuth, and M. Richardson, "OPCPA pump laser based on a regenerative amplifier with volume Bragg grating spectral filtering," Appl. Phys. B **106**, 599–603 (2012).
21. M. Hemmer, A. Vaupel, B. Webb, and M. Richardson, "Multi-kHz, multi-mJ, phase stabilized, OPCPA amplifier system," Proc. SPIE **7578**, 757818 (2010).
22. A. V. Okishev, C. Dorrer, V. I. Smirnov, L. B. Glebov, and J. D. Zuegel, "Spectral filtering in a diode-pumped Nd:YLF regenerative amplifier using a volume Bragg grating," Opt. Express **15**, 8197–8202 (2007).
23. G. Andriukaitis, T. Balčiūnas, S. Ališauskas, A. Pugžlys, A. Baltuška, T. Popmintchev, M.-C. Chen, M. M. Murnane, and H. C. Kapteyn, "90 GW peak power few-cycle mid-infrared pulses from an optical parametric amplifier," Opt. Lett. **36**, 2755–2757 (2011).
24. J. Adamonis, R. Antipenkov, J. Kolenda, A. Michailovas, A. P. Piskarskas, and A. Varanavicius, "High-energy Nd:YAG-amplification system for OPCPA pumping," Quantum Electron. **42**, 567–574 (2012).
25. W. Koechner, *Solid-State Laser Engineering* (Springer, 2006).
26. S. Seidel and N. Kugler, "Nd: YAG 200-W average-power oscillator-amplifier system with stimulated-Brillouin-scattering phase conjugation and depolarization compensation," J. Opt. Soc. Am. B **14**, 1885–1888 (1997).
27. J. Schwarz, M. Ramsey, D. Headley, P. Rambo, I. Smith, and J. Porter, "Thermal lens compensation by convex deformation of a flat mirror with variable annular force," Appl. Phys. B **82**, 275–281 (2006).
28. E. Wyss and M. Roth, "Thermooptical compensation methods for high-power lasers," IEEE J. Quantum Electron. **38**, 1620–1628 (2002).
29. L. N. Soms, A. A. Tarasov, and V. V. Shashkin, "Problem of depolarization of linearly polarized light by a YAG:Nd^{3+} laser-active element under thermally induced birefringence conditions," Sov. J. Quantum Electron. **10**, 350–351 (1980).
30. Y. Wang, K. Inoue, H. Kan, T. Ogawa, and S. Wada, "Study on thermally induced depolarization of a probe beam by considering the thermal lens effect," J. Phys. D **42**, 235108 (2009).
31. Y. Wang, K. Inoue, H. Kan, T. Ogawa, and S. Wada, "Birefringence compensation of two tandem-set Nd:YAG rods with different thermally induced features," J. Opt. A **11**, 125501 (2009).
32. W. C. Scott and M. de Wit, "Birefringence compensation and TEM00 mode enhancement in a Nd:YAG laser," Appl. Phys. Lett. **18**, 3–4 (1971).
33. N. Andreev and N. Bondarenko, "Single-mode YAG:Nd laser with a stimulated Brillouin scattering mirror and conversion of radiation to the second and fourth harmonics," Sov. J. Quantum Electron. **21**, 1045–1051 (1991).
34. M. Ostermeyer, G. Klemz, P. Kubina, and R. Menzel, "Quasi-continuous-wave birefringence-compensated single-and double-rod Nd:YAG lasers," Appl. Opt. **41**, 7573–7582 (2002).
35. D. B. Quality, N. F. Andreev, E. A. Khazanov, O. V. Kulagin, B. Z. Movshevich, O. V. Palashov, G. A. Pasmanik, V. I. Rodchenkov, A. Scott, and P. Soan, "A two-channel repetitively pulsed Nd: YAG laser operating at 25 Hz with diffraction-limited beam quality," IEEE J. Quantum Electron. **35**, 110–114 (1999).